

hep-th/9912209
 UUITP-11/99
 HIP-1999-82/TH
 December 1999

Black Hole Formation in AdS and Thermalization on the Boundary

Ulf H. Danielsson^{a,1}
 Esko Keski-Vakkuri^{a,b,2}
 Martín Kruczenski^{a,3}

^a*Institutionen för teoretisk fysik
 Box 803
 S-751 08 Uppsala
 Sweden*

^b*Helsinki Institute of Physics
 P.O. Box 9
 FIN-00014 University of Helsinki
 Finland*

Abstract

We investigate black hole formation by a spherically collapsing thin shell of matter in AdS space. This process has been suggested to have a holographic interpretation as thermalization of the CFT on the boundary of the AdS space. The AdS/CFT duality relates the shell in the bulk to an off-equilibrium state of the boundary theory which evolves towards a thermal equilibrium when the shell collapses to a black hole. We use 2-point functions to obtain information about the spectrum of excitations in the off-equilibrium state, and discuss how it characterizes the approach towards thermal equilibrium. The full holographic interpretation of the gravitational collapse would require a kinetic theory of the CFT at strong coupling. We speculate that the kinetic equations should be interpreted as a holographic dual of the equation of motion of the collapsing shell.

¹E-mail: ulf@teorfys.uu.se

²E-mail: esko.keski-vakkuri@hip.fi ^b Permanent address.

³E-mail: martink@teorfys.uu.se

1 Introduction

Following the discovery of the AdS/CFT correspondence [1] a large amount of work has been devoted to clarifying and extending its implications. This work has been recently reviewed in [2] where an extensive list of references can be found. In this context, we have investigated [3, 4, 5] the relation between physics in the bulk of AdS and its holographic dual. We have mainly focused on the formulation in Minkowski signature [6, 7] since this allows the study of dynamical processes. In particular we have been interested in the holographic interpretation of black hole formation in the bulk since the full understanding of this process is an important step towards the ultimate goal of finding a holographic interpretation of the black hole information problem [8], and (hopefully) its solution. We also believe that by investigating the formation of black holes one will gain a deeper understanding of general features of holography. The process that we are focusing on is the spherical collapse of a thin shell of unspecified matter in the bulk. A special case, the spherical collapse of a dust shell in AdS_3 , was analyzed by Peleg and Steif in [9]⁴. In the holographic dual, a flat space field theory with no gravity, the bulk process is expected to correspond to the time evolution and thermalization of an initial out of equilibrium state [7, 11, 12, 13]. The collapse of the shell due to gravity describes the approach towards equilibrium, while the final formation of the black hole corresponds to thermalization. It is intriguing how a gravitational process in the bulk is encoded in a kinetic process in the holographic dual. This, we believe, suggests a deep connection through holography between gravity and kinetic theory of the boundary theory.

In [4] we developed Green function techniques that allowed us to obtain the holographic “images” of various objects in the bulk. In [5] we used these techniques to begin our study of black hole formation. As a first step we studied the case of a very large shell of matter which is just beginning to collapse. In this case we could neglect the motion of the shell and use a quasistatic approximation. The motivation for the study was to find out how the scale-radius duality [7, 12, 15, 16] encodes the radial size of a spherically symmetric shell, and to find properties of the off-equilibrium state in the holographic dual. We found that the presence of the shell manifested itself in the form of a series of poles in the propagator. The location of these poles depends on the radius of the shell, in agreement with the scale-radius duality. A slight surprise was that the poles also had an imaginary part. Hence they can be interpreted as unstable collective excitations, “shellons” (since they exist because of the shell), in the off-equilibrium state.

In this paper we will carry the analysis one step further. While we are not yet able to address the time-dependence of the collapse, there is another regime where a quasistatic

⁴The other extreme case, collapse of a solid disk of dust in AdS_3 was investigated by Mann and Ross in [10].

approach can again be adopted: the very last stage when the shell is approaching the horizon radius r_H of the black hole about to form. There are two ways to justify the quasistatic approximation.

First, in the final stage of the gravitational collapse the shell appears to “freeze” in the frame of an asymptotic observer. The approach of the radius of the shell r_s to the radius of the horizon r_H is exponentially slow,

$$\frac{r_s - r_H}{r_H} \sim e^{-t/\tau_H} , \quad (1)$$

where the characteristic timescale τ_H is inversely proportional to the Hawking temperature⁵,

$$\tau_H = \frac{1}{4\pi T_H} . \quad (2)$$

Therefore, the quasistatic approximation is applicable for evaluating the propagator as long as we focus on energies which are larger than the inverse characteristic timescale,

$$|\omega| > \frac{1}{\tau_H} \sim T_H . \quad (3)$$

At the same time, this is the region of interest for investigating the approach to thermal equilibrium. At equilibrium, the propagator becomes thermal, with a characteristic infinite sequence of thermal poles

$$\omega_n = i4\pi n T_H + \text{const.} , \quad n = \pm 1, \pm 2, \dots . \quad (4)$$

When the radius of the shell is slightly larger than the horizon radius, the boundary theory is slightly out of equilibrium, and one finds a correction factor to the thermal propagator which has additional (shellon) poles and zeroes. They characterize the deviation from the equilibrium; the poles and zeroes flow together and disappear during the approach to equilibrium.

Second, one can avoid the restriction to large frequencies by investigating a slightly different way of approaching the equilibrium. In the bulk one can consider a sequence of static spherical shells with a constant total ADM mass, but with progressively smaller radii approaching the horizon radius. Instead of starting with a shell at rest and letting it collapse freely, this corresponds to slowing down the collapse by applying an external force so that the process becomes quasistatic, while increasing the amount of matter in the shell. The ADM energy needs to be kept fixed to ensure that the shell approaches its horizon radius, therefore the loss of kinetic energy needs to be compensated by adding matter to the shell during the process. In this case one obtains more detailed information

⁵This is true for the production of a generic black hole in a generic dimension.

about the propagator in the boundary theory. Presumably, the quasistatic approximation amounts in the boundary theory to replace the kinetic theory by a thermodynamical treatment of small deviations from equilibrium. In thermodynamics the evolution of a system is always considered to be quasistatic, and small deviations from equilibrium can be arranged to be such by applying external forces. The evolution is then determined by the gradient of entropy depending on a small parameter characterizing the deviation from equilibrium, which should correspond to the applied force balancing the gravitational force in the bulk. In contrast, recently [14] the equations of motion in the bulk were related to renormalization group equations in the boundary. This is a good interpretation for the static background geometry but general relativity also determines the time evolution of an object in the bulk – this is a dynamical process related to the dynamics of the boundary as discussed above.

The paper is organized as follows. In section 2 we review our previous work and compare our results with other recent work on black hole formation [17, 18, 19, 20]. The analysis of the last stages of black hole formation in the case of AdS_3 is given in section 3. Section 4 contains a discussion of results and some ideas for the future.

2 Derivation of the correlators

We begin by briefly reviewing (following [21, 22] and as described in [5]) the essential steps of the computation of a two point function of a boundary operator coupling to a bulk scalar field in an asymptotically AdS spacetime. A scalar field in the bulk satisfies the classical equation of motion

$$\left[\frac{1}{\sqrt{-g}} \partial_\mu \sqrt{-g} g^{\mu\nu} \partial_\nu - m^2 \right] \phi(t, \vec{x}, r) = 0 \quad (5)$$

where $g_{\mu\nu}$ is the bulk metric and the mass term m^2 contains the mass of the field, the coupling to the curvature scalar⁶, and contributions from a Kaluza-Klein reduction on a compact internal space, if the original spacetime is higher dimensional. At first, we choose the desired coordinate system for (a part of) AdS space. We will work in Minkowski signature. Depending on the choice of coordinates, we then impose the appropriate boundary condition for the bulk field in the interior. For example, in AdS with global coordinates one requires that ϕ vanishes at the origin. In Poincaré coordinates or in the case of a black hole, the appropriate boundary condition at the horizon is an ingoing wave when the imaginary part of the energy is positive and an outgoing when it is negative. The

⁶When we consider *e.g.* a spacetime of a collapsing shell in AdS_{d+1} with $d > 2$, the exterior metric has a nonconstant scalar curvature. In such cases we assume that the scalar field is minimally coupled so that m^2 remains a constant.

propagator then has a cut on the real axis where the imaginary part changes sign. Let t, \vec{x} denote the coordinates that parametrize the boundary, and let r denote the radial coordinate. We perform a Fourier transformation to momentum space in the boundary coordinates, so the interior solution is $\phi(\omega, \vec{k}, r)$. This solution is uniquely determined (up to an overall normalization) by the boundary conditions discussed above.

We then study its behavior near the boundary. In Minkowski signature, there are two kinds of bulk field modes, normalizable and non-normalizable⁷. In momentum space, we denote the former by $\phi^{(+)}(\omega, \vec{k}, r)$ and the latter by $\phi^{(-)}(\omega, \vec{k}, r)$. We normalize the modes such that their asymptotic behavior near the boundary is

$$\phi^{(\pm)}(\omega, \vec{k}, r) = r^{-\Delta_{\pm}} \cdot 1 \quad (r \rightarrow \infty) \quad (6)$$

where

$$\Delta_{\pm} = \frac{1}{2}(d \pm \sqrt{d^2 + 4m^2}) \equiv \frac{d}{2} \pm \nu . \quad (7)$$

Now, in the asymptotic region, the interior solution $\phi(\omega, \vec{k}, r)$ becomes a linear combination of the normalizable and non-normalizable solutions, with an asymptotic behavior

$$\phi(t, \vec{x}, r) \approx r^{-\Delta_+} C(\omega, \vec{k}) + r^{-\Delta_-} D(\omega, \vec{k}) . \quad (8)$$

The coefficient $D(\omega, \vec{k})$ is the Fourier transform of the boundary data $\phi_0(t, \vec{x})$ which acts as a source term for a dimension Δ_+ operator $\mathcal{O}(t, \vec{x})$ in the boundary theory [21, 22]. Next, we rewrite (8) in the form

$$\phi(\omega, \vec{k}, r) \approx \left[r^{-\Delta_+} G(\omega, \vec{k}) + r^{-\Delta_-} \right] \phi_0(\omega, \vec{k}) , \quad (9)$$

where

$$G(\omega, \vec{k}) = \frac{C(\omega, \vec{k})}{D(\omega, \vec{k})} . \quad (10)$$

One can then check that the (finite part) of the two point function of the operator \mathcal{O} at the boundary has the momentum space form⁸

$$\langle \mathcal{O}(\omega, \vec{k}) \mathcal{O}(\omega', \vec{k}') \rangle = \left(\frac{\Delta_+ - \Delta_-}{2} \right) \delta(\omega + \omega') \delta(\vec{k} + \vec{k}') G(\omega, \vec{k}) . \quad (11)$$

In the case that the geometry has a horizon, the propagator, as a function of the frequency ω , has a cut on the real axis which arises from the boundary conditions as we already discussed. In that case one can analytically continue the propagator from the

⁷The Minkowski signature version of AdS/CFT duality was first investigated in [6, 7].

⁸The evaluation of the overall coefficient involves a subtlety, see [23]. In the remainder of the paper we will suppress overall coefficients as they do not affect the pole structure of the propagator.

upper half-plane into the lower half-plane. This analytic continuation can have poles on the lower half plane signaling the presence of unstable quasi particles.

Next, we compute the propagator in the presence of a thin matter shell of radius r_s in AdS_{d+1} space. We are going to restrict attention to a quasistatic approximation: we assume that the shell is collapsing very slowly (as measured in the asymptotic time), so that it appears to be static⁹. The static case has an interest also of its own since it provides a series of states which are closer and closer to equilibrium. Understanding how these states differ from the black hole from the boundary point of view, gives an insight into the boundary processes at work. Furthermore, the usual thermodynamical approach to out of equilibrium states is to consider states which are at equilibrium but for a variable that is externally kept fixed. In this case the variable is the radius of the shell.

In the interior of the shell, the metric is the AdS metric in global coordinates, and the exterior metric is the AdS black hole metric. Both metrics can be expressed in the form

$$ds^2 = -f(r)dt^2 + \frac{dr^2}{f(r)} + r^2d\Omega_{d-1} , \quad (12)$$

with the function $f(r)$:

$$f(r) = \begin{cases} f_1(r) = 1 + r^2 & \text{if } r < r_s \\ f_2(r) = 1 - \frac{\mu}{r^{d-2}} + r^2 & \text{if } r > r_s \end{cases} , \quad (13)$$

where the parameter μ is related to the ADM mass of the black hole. The radius of the horizon of the black hole, r_H , is determined by solving the equation $f_2(r_H) = 0$. (We are using units where t, r and the angular coordinates are dimensionless and the AdS radius is set to $R = 1$. The dimensions can be restored by replacing everywhere $r \rightarrow r/R$ etc. With the metric (12), the scalar field equation (5) can be reduced (after a Fourier transformation to momentum space in the boundary coordinates) to the radial equation

$$\frac{1}{r^{d-1}}\partial_r \left(r^{d-1}f(r)\partial_r \right) \phi(\omega, \vec{k}, r) + \left(\frac{\omega^2}{f(r)} - \frac{k^2}{r^2} - m^2 \right) \phi(\omega, \vec{k}, r) = 0 , \quad (14)$$

where $k^2 = l(l + d - 2)$, $l = 0, 1, 2, \dots$ is the eigenvalue of the Laplacian on the $(d - 1)$ -sphere. The interior and exterior solutions ϕ_1 and ϕ_2 of the radial equation must be matched across the thin shell using flux conservation. The matching conditions are

$$\phi_1|_{r=r_s} = \phi_2|_{r=r_s} \quad (15)$$

$$f_1(r)\partial_r\phi_1|_{r=r_s} = f_2(r)\partial_r\phi_2|_{r=r_s} . \quad (16)$$

⁹Of course, a complete treatment should take into account what happens when the shell is collapsing rapidly. This can be expected to give rise to particle production in the boundary theory even if we neglect the particle production in the bulk. We will leave these more demanding issues aside here.

To find the propagator $G(\omega, \vec{k})$ in the boundary, we first expand the exterior solution in normalizable and non-normalizable modes,

$$\phi_2(\omega, \vec{k}, r) \approx r^{-\Delta+} C(\omega, \vec{x}) + r^{-\Delta-} D(\omega, \vec{k}) , \quad (17)$$

then substitute (17) in the matching conditions above, solve for the ratio C/D in terms of ϕ_1 and ϕ_2 , and substitute into equation (10) which gives the propagator. The result is

$$G(\omega, \vec{k}) = -\frac{\phi_1 f_2 \partial_r \phi_2^{(-)} - \phi_2^{(-)} f_1 \partial_r \phi_1}{\phi_1 f_2 \partial_r \phi_2^{(+)} - \phi_2^{(+)} f_1 \partial_r \phi_1} . \quad (18)$$

In the above, all quantities are evaluated at the radius of the shell r_s . The analytic structure of the resulting propagator gives information about the spectrum of excitations in the boundary theory. In particular, we are interested in the poles of the propagator at zero transverse momentum ($\vec{k} = 0$) in the complex ω -plane. Poles at positive real ω -axis correspond to masses of stable composite objects created and annihilated by \mathcal{O} . However, we will typically find complex poles at

$$\omega_n = M_n - \frac{i}{2} \Gamma_n \quad (19)$$

corresponding to unstable resonances created and annihilated by \mathcal{O} . In a previous paper[5], we used the name “shellons” for the resonances. The real part M_n gives the mass of the resonance, and the imaginary part Γ_n is the width which is the inverse of the lifetime. There can also be poles in the imaginary ω -axis, for example when the black hole has fully formed and the boundary theory has thermalized. Then the boundary propagator becomes a thermal propagator, and the imaginary poles are related to periodicity in imaginary time.

From (18), we see that the poles typically correspond to the zeroes of the denominator (unless they cancel against those of the numerator). The vanishing of the denominator means that the interior solution ϕ_1 matches completely with a normalizable exterior solution $\phi_2^{(+)}$. Thus, the total mode is normalizable – unless ω is complex, in which case it will be quasinormalizable. For a better understanding of the situation, it is instructive to map the radial equation into the form of a Schrödinger equation and consider the resulting quantum mechanical analogue. We rescale the field ϕ as

$$\phi(\omega, \vec{k}, r) = r^{(-d+1)/2} \psi(\omega, \vec{k}, r) \quad (20)$$

and use a “tortoise” coordinate

$$r_* = \int \frac{dr}{f(r)} . \quad (21)$$

Note that we have to use f_1 in the interior and f_2 in the exterior, so we must add an integration constant to ensure that r_* is continuous across the shell. The range of r_* is finite. For example, if $d = 2$, we get

$$r_* = \begin{cases} -\frac{1}{2r_H} \ln \left(\frac{r+r_H}{r-r_H} \right) & r > r_s \\ \arctan(r) - r_0 & 0 \leq r < r_s \end{cases} \quad (22)$$

where

$$r_0 = \arctan(r_s) + \frac{1}{2r_H} \ln \left(\frac{r_s + r_H}{r_s - r_H} \right) \quad (23)$$

and the full range of r_* is the finite interval $-r_0 \leq r_* \leq 0$. In the following we will mostly be considering the case where the radius of the final black hole, r_H , and therefore also the radius of the shell, r_s , are very large compared to the AdS radius ($r_s > r_H \gg 1$ in our units). The radial equation in the interior will then reduce to that in a Poincaré patch of AdS space (see [5]), and the two equations above become

$$r_* = \begin{cases} -\frac{1}{2r_H} \ln \left(\frac{r+r_H}{r-r_H} \right) & r > r_s \\ -\frac{1}{r} - r_0 & 0 \leq r < r_s \end{cases} \quad (24)$$

where

$$r_0 = \frac{1}{2r_H} \ln \left(\frac{r_s + r_H}{r_s - r_H} \right) - \frac{1}{r_s} . \quad (25)$$

The full range of r_* is now the infinite interval $-\infty \leq r_* \leq 0$, corresponding to the infinite AdS throat.

With the above rescalings, the radial equation (14) reduces to the form of a time independent Schrödinger equation,

$$-\partial_{r_*}^2 \psi + V(r_*) \psi = \omega^2 \psi \quad (26)$$

with a potential

$$V(r_*) = \frac{(d-1)(d-3)f^2}{4r^2} + \frac{(d-1)\partial_{r_*} f}{2r} + \frac{(k^2 + m^2 r)f}{r} , \quad (27)$$

where $r = r(r_*)$ from inverting (21) and $f = f(r(r_*))$. Thus the problem of solving the radial equation becomes analogous to a one dimensional quantum mechanical scattering problem. In Figure 1 a typical profile of the potential is depicted. It blows up at the boundary and has a small barrier at the location of the shell¹⁰. There is also an infinite well at $r_* = -r_0$, but when we consider a large black hole the well is pushed down the

¹⁰If we were relax the quasistatic approximation and allow for the time dependence of the collapsing shell, we would need to consider quantum mechanical scattering with a time dependent potential: the barrier would be moving to the left.

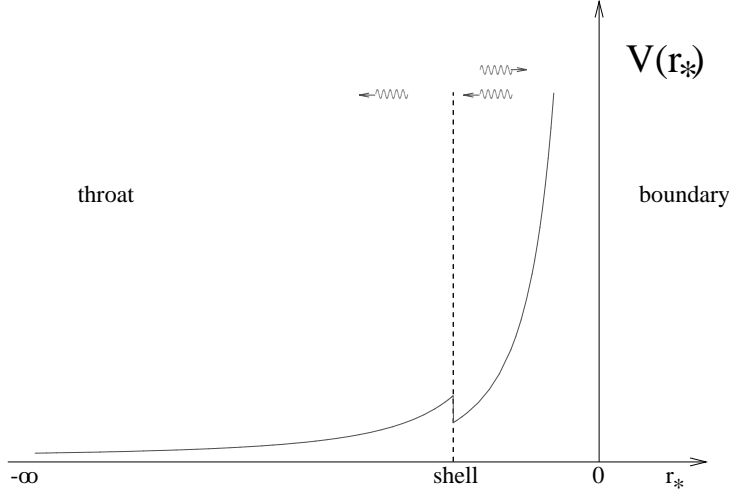


Figure 1: Potential in the presence of a shell.

AdS throat towards $r_* = -\infty$ and plays no role in the calculation. Now let us return to the poles of (18). As we discussed above, the appropriate interior boundary condition for ϕ_1 is that it is a purely ingoing wave. On the other hand, the normalizable mode in the exterior is a superposition of an outgoing wave and an ingoing wave, due to the reflection from the boundary of AdS. For example, it is simple to check this by looking at the high frequency limit of the normalizable mode $\phi_2^{(+)}$ [3, 5], which looks like

$$\phi_2 \approx r^{(-d+1)/2} \cos\left(\frac{\omega}{r} + \theta_0\right) \quad (28)$$

where θ_0 is a constant phase shift. For the “wavefunction” ψ this means that it is a superposition of ingoing and outgoing waves with *equal amplitude* on the right hand side of the barrier corresponding to the shell (see Figure 1) and on the left hand side there is a purely ingoing wave. Thus there is total reflection together with transmission – it is impossible to satisfy both conditions with real energy levels. However, it is possible with *complex* energy levels ω^2 . This is another way to see why the poles appear at complex frequencies ω . Incidentally, note that using the tortoise coordinate (21), the propagator (18) takes an even simpler form – it is just a ratio of two Wronskians

$$G(\omega, \vec{k}) = -\frac{W(\phi_1, \phi_2^{(-)})}{W(\phi_1, \phi_2^{(+)})} \quad (29)$$

evaluated at $r_* = r_*(r_s)$.

Let us compare our approach with other recent work. Horowitz and Hubeny [19] investigated the quasinormal modes in the background of a black hole¹¹. They study the equation (14) with the black hole metric ($f(r) = f_2(r)$). The boundary conditions in [19] for a scalar field are very similar to ours: one takes the field to be a superposition of outgoing and ingoing modes near the boundary (normalizable modes), whereas the interior boundary condition in [19] is that there should be only ingoing modes near the horizon of the black hole. In our case with a shell, the interior metric is that of a pure AdS space. However, if the radius of the shell is larger than the AdS space ($r_s \gg 1$ in the present units), a Poincaré horizon appears at $r \rightarrow 0$ ($r_* = -\infty$) due to the approximation, and there is a natural choice between ingoing or outgoing modes, which is reflected in a cut appearing in the propagator¹² of the boundary operator \mathcal{O} . Thus, on a formal level the modes we discussed in [5] are analogous to the quasinormal modes of black holes [19]. The complex spectrum arises because of the choice of boundary conditions, and the main difference between [19] and [5] is that the horizon of a black hole has been replaced by a Poincaré horizon. However, the physical interpretation appears to be somewhat different. The horizon of a black hole is a real boundary through which matter can fall in and be lost, while the appearance of a Poincaré horizon in the above is merely an artifact of the approximation since we started from global AdS space. In reality we would expect an ingoing wave to be reflected back from the origin of the AdS space and not to be lost. What happens is that if the radius of the shell is much larger than the AdS radius, $r_s \gg 1$, and the frequency is complex (with $\Im\omega < 0$) the reflection is exponentially attenuated, so that it can be suppressed. There are two other ways to arrange for the ingoing mode from the shell not to come back at all. One way is simply to consider a shell falling into an existing (small) black hole instead of creating the black hole in the collapse. Another way is to consider late times in the collapse when the shell is approaching the radius of the horizon of the black hole about to be created. From the space-time diagram of black hole formation in a spherical collapse, one can see that the horizon forms even before the black hole has formed. Therefore, the ingoing modes from the shell will be lost into the region of trapped surfaces and never come back.

Another related work is by Giddings and Ross [18] who investigated a collapsing shell of D-branes. In their case, contrary to ours with an unspecified matter shell in AdS space, the geometry in the interior of the D-brane shell is flat. Hence they do not have an infinite throat, where objects falling in could get lost. Instead, their space is cut off at a finite r_* . As a consequence, when they investigate the poles of the propagator, they initially obtain a discrete spectrum of stable excitations with real energies, much like the global modes in

¹¹Related work can be found in [24].

¹²The choice between the two sides of the cut corresponds to a choice between a retarded or advanced propagator.

our case. However, the shell itself can absorb incoming waves, and after considering this effect they also obtain imaginary contributions to the energy spectrum. So the absorption by the shell plays a similar role as the absorption by the infinite throat in AdS space in our case.

Furthermore, Balasubramanian and Ross [17] have investigated black hole formation in AdS_3 by point particles. The bulk solution was investigated by Matschull [25], and Balasubramanian and Ross investigate the use of 2-point functions in the boundary theory to keep track of the positions of the point particles as they approach each other. In this case one does not have the complication of spherical symmetry, the point particle positions can be read off from kinks in the 2-point functions in *coordinate* space.

Finally, we would like to mention a slightly different line of work on thermalization in the context of black holes and AdS/CFT correspondence. Kiritis and Taylor [26] investigated D-brane probes falling into a black hole. In the process, the potential energy of the probe is converted into heat, which then is absorbed by the black hole. By investigating the bulk action of the probe, one can *e.g.* derive the equation of state for the black hole. But, on the other hand, one can study the dual gauge theory effective action of the probe at finite temperature and try to reproduce predictions from bulk calculations; this was investigated in [27].

3 Black hole formation in AdS_3

In this section we examine the boundary propagator in the case that a shell is quasistatically forming a black hole in AdS_3 space. As in [5], we assume that the resulting black hole has a much larger radius than that of the AdS space: $r_H \gg 1$ in the present units. The problem is to find the modes $\phi_1, \phi_2^{(\pm)}$ which are needed in the propagator formula (18). To find the interior mode, note that in the region $r > r_s \gg 1$ we can approximate $f_1(r) = 1 + r^2 \approx r^2$. Then the radial equation becomes the mode equation in Poincaré coordinates, and the mode solutions will be Bessel functions $\phi \sim (1/r) J_{\pm\nu}(\sqrt{\omega^2 - k^2}/r)$. As discussed in section 2, in Poincaré coordinates the natural choice for the interior boundary condition is between ingoing and outgoing modes, and we choose the former, as we did in [5]. However, in [5] we made an additional approximation and focused on the large frequency limit $\omega/r \gg 1$. Here we will not make that approximation, so the infalling mode is the following linear combination

$$\phi_1 = c_1 \frac{1}{r} \left(J_\nu \left(\frac{\sqrt{\omega^2 - k^2}}{r} \right) - e^{i\pi\nu} J_{-\nu} \left(\frac{\sqrt{\omega^2 - k^2}}{r} \right) \right), \quad (30)$$

where $\nu = \sqrt{1 + m^2}$ and c_1 is a normalization constant (which will drop out in the answer for the propagator).

Then, we need the exterior modes $\phi_2^{(\pm)}$ in BTZ coordinates. In our previous paper [5], we used a WKB approximation in the large frequency limit to obtain the modes. Here, we will instead use the exact solutions of the wave equation [28], the normalizable and nonnormalizable modes can be found in [3]. If the shell is large ($r_s \gg r_0$), we use

$$\phi_2^{(\pm)} = (u - 1)^\alpha u^{-(\Delta_\pm/2) - \alpha} F\left(\alpha + \frac{\Delta_\pm}{2}, \alpha + \frac{\Delta_\pm}{2}; 1 + \nu; u^{-1}\right), \quad (31)$$

where $u = r^2/r_H^2$, $\alpha = i\omega/(2r_H)$ and Δ_\pm were defined in (7). Substituting (30) and (31) into (18), we obtain the result for the propagator of the operator \mathcal{O} on the boundary in the presence of a large matter shell in the bulk. Using the latter result we checked that we reobtain our previous approximate result for the poles in the $r_s \gg r_H$, $\omega \gg r_s$ limit:

$$\omega_n = \pi r_s \left(n + \frac{3}{4} + \frac{\nu}{2} \right) - \frac{ir_s}{2} \ln \left(\frac{4\pi n r_s^2}{r_H^2} \right). \quad (32)$$

This is sufficient to illustrate the main point: the presence of the spherically symmetric shell in the bulk is encoded in a tower of resonances in the boundary theory, with the above spectrum from which one can read their masses and decay widths. An intriguing thing about the shellon poles becomes apparent if we focus on the UV limit $|\omega| \gg 1$. By the scale-radius duality one might have thought that we in the bulk are probing only the geometry very near the boundary. But that is a region outside of the shell, so the geometry is equal to the black hole geometry. On the other hand, near the boundary the black hole metric reduces to the same form as the Poincaré metric. From these arguments we might have expected that the analytic structure of the propagator in the UV limit is either similar to that of the thermal propagator, or the Poincaré propagator¹³. On the other hand, from (32) we know that there are poles for arbitrary large ω arising from the shell. A possible interpretation is that the poles of the propagator do not only carry local information about the geometry of spacetime near the boundary - they also carry information about an event that happens deep in the bulk inside the shell: the absorption of the ingoing wave into the (fictitious) horizon, which was used as a boundary condition in the evaluation of the propagator.

Rather than present more details and more accurate results for the poles in the large shell case, we turn our attention to the other extreme of the collapse of the shell: the approach to the horizon radius ($(r - r_H)/r_H \ll 1$) where we expect to see thermalization on the boundary.

As the shell is approaching the horizon, we choose the following expressions for the exterior normalizable and nonnormalizable modes [3]:

$$\phi_2^{(\pm)} = A_\pm (u - 1)^\alpha F\left(\alpha + \frac{\Delta_\pm}{2}, \alpha + \frac{\Delta_\mp}{2}; 2\alpha + 1; 1 - u\right)$$

¹³We would like to thank Per Kraus and Sandip Trivedi for pointing out this issue to us.

$$+ B_{\pm}(u-1)^{-\alpha}F(-\alpha+\frac{\Delta_{\pm}}{2}, -\alpha+\frac{\Delta_{\mp}}{2}; -2\alpha+1; 1-u) , \quad (33)$$

where

$$A_{\pm} = \frac{\Gamma(1 \pm \nu)\Gamma(-2\alpha)}{\Gamma^2(-\alpha + \frac{\Delta_{\pm}}{2})} \quad (34)$$

$$B_{\pm} = \frac{\Gamma(1 \pm \nu)\Gamma(2\alpha)}{\Gamma^2(\alpha + \frac{\Delta_{\pm}}{2})} . \quad (35)$$

and we used α as defined in (31). We then plug the interior mode (30) and the exterior modes (33) into the main propagator formula (18), and study its analytic structure. To simplify matters, we again focus on the propagator at zero transverse momentum, $G(\omega, k = 0)$.

Let us begin with some general observations. As the shell approaches the horizon, the boundary theory gets closer and closer to thermal equilibrium. Therefore, in the limit $r_s \rightarrow r_H$, $G(\omega, k)$ should become the thermal propagator which we evaluated in our previous work [5]. The thermal propagator (which we denote by $G_T(\omega, k)$ from now on) has a characteristic infinite sequence of zeroes and poles, at zero momentum they are located on the imaginary axis on the complex ω -plane. Before the limit $r_s \rightarrow r_H$, when the shell is at a small distance from the horizon, the boundary theory is slightly off thermal equilibrium. In that case, we find it useful to write the propagator in a factorized form

$$G(\omega, k = 0) = G_T(\omega, k = 0) \times H(\omega, k = 0) , \quad (36)$$

This is useful for two reasons. First, if $r_s \rightarrow r_H$ and $\text{Im}\omega > 0$, then $H(\omega, k = 0) \rightarrow 1$ and H encodes small deviations from the thermal equilibrium when $r_s \neq r_H$. Second, when $\text{Im}\omega < 0$, $H(\omega, k = 0)$ has poles which are then poles of the propagator. The expression can be misleading if used on, for example, the imaginary axis, since G_T has poles at $\omega = -i4\pi n T_H$ (T_H is the temperature of the black hole) whereas G does not since they are canceled by H . These thermal poles appear in G only after taking the limit $r_s \rightarrow r_H$. Formally one has to consider $\text{Im}\omega > 0$, take the limit $r_s \rightarrow r_H$ in which case $H(\omega, k = 0) \rightarrow 1$, and then analytically continue below the real axis. Since then $G = G_T$ they also have the same poles. The analytic continuation is necessary since when $r_s \rightarrow r_H$ a new cut arises as an accumulation of poles and zeros. In fact it can be said that the cut due to the boundary conditions at the Poincaré horizon is replaced by another one due to the new boundary conditions at the horizon of the black hole which forms.

After discussing this point, we try to analyze the propagator without any approximations for the interior and exterior modes (30) and (33). We assume that we are initially on the upper half ω -plane. Then, one can see that the leading terms of the exterior modes

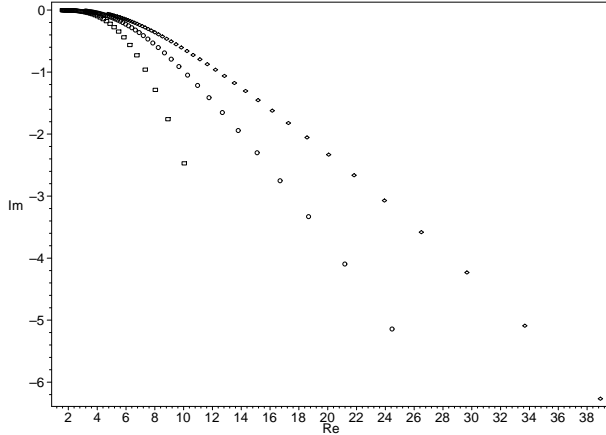


Figure 2: Flow of the first three poles of H in the complex ω plane as the shell contracts towards the horizon. In the numerical calculation, we used the parameter values $\nu = 1.5$, $r_H = 10$ (horizon radius), and the initial radius of the shell is $r_s = 10.25$.

(33) have a coefficient A_{\pm} . We can pull out these coefficients in the numerator and denominator of G , whereafter they will give us the “thermal” factor G_T . In other words, now

$$G_T(\omega, 0) = -\frac{A_-}{A_+} = -\left(\frac{\Gamma(-\frac{i\omega}{4\pi T} + \frac{\Delta_{\pm}}{2})}{\Gamma(-\frac{i\omega}{4\pi T} + \frac{\Delta_{\mp}}{2})}\right)^2 \quad (37)$$

and

$$H(\omega, 0) = \frac{\phi_1 f_2 \partial_r (\phi_2^{(-)} / A_-) - (\phi_2^{(-)} / A_-) f_1 \partial_r \phi_1}{\phi_1 f_2 \partial_r (\phi_2^{(+)} / A_+) - (\phi_2^{(+)} / A_+) f_1 \partial_r \phi_1} \quad (38)$$

The “correction factor” $H(\omega, 0)$ is too complicated to allow us to find an analytic expression for the poles. Therefore we have evaluated them numerically, using Maple V version 5. Figure 2 below depicts the flow of the first couple of poles of H as the shell radius r_s approaches the horizon radius r_H . Numerical investigations tell us that the poles of H start out in the lower half complex ω -plane (where the poles were found as the shell was still large), and then move towards the real axis and the origin. Specifically, as r_s is sufficiently close to r_0 , the real and imaginary parts of the poles ω become much smaller than r_H, r_s . Further, the imaginary part decreases more rapidly than the real part, and quickly becomes many orders of magnitude smaller. This is illustrated in Table 1 below which lists a few characteristic values for a pole as r_s approaches r_H .

r_s	ω
10.25	10.04-2.47i
10.016	6.76-0.73i
10.0020	5.49-0.35i
10.00024	4.65-0.18i
10.000031	4.03-0.10i
10.0000020	3.43-0.049i
10.00000024	3.08-0.030i
10.000000030	2.80-0.019i

Table 1. Pole values ω as r_s approaches $r_H = 10$. (Using $\nu = 1.5$.)

We now turn to search for a simplified expression for H , and begin by making some approximations for the interior and exterior modes. Let's first consider the exterior modes $\phi_2^{(\pm)}$. As $(r_s - r_H)/r_H$ becomes small, $u = r_s^2/r_H^2$ approaches 1 and we can do a series expansion in $(u - 1)$ obtaining

$$\phi_2^{(\pm)} \approx \left\{ A_{\pm} \left[(u - 1)^{\alpha} + \mathcal{O}((u - 1)^{\alpha+1}) \right] + B_{\pm} \left[(u - 1)^{-\alpha} + \mathcal{O}((u - 1)^{-\alpha+1}) \right] \right\}. \quad (39)$$

Similarly, we obtain a series expansion for the combination $f_2 \partial_r \phi_2^{(\pm)}$ which also appears in the equation (18) for the propagator,

$$f_2 \partial_r \phi_2^{(\pm)} \approx 2r \left\{ A_{\pm} \left[(u - 1)^{\alpha} + \mathcal{O}((u - 1)^{\alpha+1}) \right] - B_{\pm} \left[(u - 1)^{-\alpha} + \mathcal{O}((u - 1)^{-\alpha+1}) \right] \right\}. \quad (40)$$

Recalling that $\alpha = i\omega/(2r_H)$ it immediately follows that $(u - 1)^{\alpha}$ is the leading term if $\text{Im}\omega > 0$ whereas $(u - 1)^{-\alpha}$ dominates for $\text{Im}\omega < 0$. Replacing in equation (18) results in

$$\lim_{r_s \rightarrow r_H} G(\omega, r_s) = \begin{cases} -\frac{A_-}{A_+} & \text{if } \text{Im}\omega > 0 \\ -\frac{B_-}{B_+} & \text{if } \text{Im}\omega < 0 \end{cases} \quad (41)$$

Note that independently of the function ϕ_1 , i.e. independently of the boundary conditions at the Poincaré throat, the propagator develops a cut with the right boundary conditions at the horizon of the black hole. At the cut the imaginary part of the propagator changes sign since $A_{\pm} = B_{\pm}^*$.

After checking that in the limit $r_s \rightarrow r_H$ the propagator reduces to the black hole propagator, we proceed to compute the corrections when r_s is close but not equal to r_H . It is easy to see that if the dominant term is for example $(u - 1)^{\alpha}$ then no corrections are obtained from keeping terms of order $(u - 1)^{\alpha+n}$ unless the term $(u - 1)^{-\alpha}$ is included. The same occurs when $\text{Im}\omega < 0$ and $(u - 1)^{-\alpha}$ dominates. Therefore, to compute the

corrections we use the approximations

$$\phi_2^{(\pm)} \approx \left\{ A_{\pm}(u-1)^{\alpha} + B_{\pm}(u-1)^{-\alpha} \right\} \quad (42)$$

$$f_2 \partial_r \phi_2^{(\pm)} \approx 2r\alpha \left\{ A_{\pm}(u-1)^{\alpha} - B_{\pm}(u-1)^{-\alpha} \right\} \quad (43)$$

in the equation for the propagator.

With the above approximations, the expression for the correction factor H becomes

$$H(\omega, 0) \approx \frac{\left[\frac{i\omega}{r_H} - a \right] (u-1)^{\alpha} - \left[\frac{i\omega}{r_H} + a \right] \frac{B_-}{A_-} (u-1)^{-\alpha}}{\left[\frac{i\omega}{r_H} - a \right] (u-1)^{\alpha} - \left[\frac{i\omega}{r_H} + a \right] \frac{B_+}{A_+} (u-1)^{-\alpha}}, \quad (44)$$

where $a \equiv \partial_r \ln \phi_1$. With this expression it is very easy to see that there are no poles in G . In the upper half plane, where the imaginary part of ω is positive, α is negative and $G \rightarrow -\frac{A_-}{A_+}$ as $r_s \rightarrow r_H$, $(u \rightarrow 1)$. This expression has no poles where it is valid, i.e. in the upper half plane. Similarly, in the lower half plane we have $G \rightarrow -\frac{B_-}{B_+}$ which again has no poles where it is valid. Let us now return to H . To find the zeroes and poles of H , we have to solve for the values of ω where the numerator or the denominator vanishes.

We aim here to confirm what we saw numerically before, namely that the poles and zeros accumulate on the real axis giving rise to a cut. In that case what has to happen is that the poles go to zero as $r_s \rightarrow r_H$ (see appendix for an example). To check this fact we only need to study the propagator for frequencies such that $\omega/r_s \ll 1$ which is fortunate since in that regime the equations simplify¹⁴ in two ways. First, the mode in the interior of the shell, ϕ_1 can be expanded as:

$$\phi_1 \approx \frac{1}{\sqrt{r}} \left\{ \frac{(\omega/2r)^{\nu}}{\Gamma(\nu+1)} - \frac{(\omega/2r)^{\nu+2}}{\Gamma(\nu+2)} + \cdots - e^{i\pi\nu} \left[\frac{(\omega/2r)^{-\nu}}{\Gamma(-\nu+1)} - \frac{(\omega/2r)^{-\nu+2}}{\Gamma(-\nu+2)} + \cdots \right] \right\}. \quad (45)$$

Keeping only the leading term when $\omega/r_s \ll 1$ it follows that

$$\phi_1 \approx -e^{i\pi\nu} \frac{(\omega/2)^{-\nu}}{\Gamma(-\nu+1)} r^{-\nu-\frac{1}{2}} \Rightarrow a = \partial_r \ln \phi_1 = \nu - \frac{1}{2}. \quad (46)$$

Furthermore, we are able to do one more approximation:

$$\begin{aligned} \frac{B_{\pm}}{A_{\pm}} &= \frac{\Gamma(2\alpha)\Gamma^2(-\alpha + \Delta_{\pm}/2)}{\Gamma(-2\alpha)\Gamma^2(\alpha + \Delta_{\pm}/2)} \\ &\approx -1 + 2i[\psi(\frac{\Delta_{\pm}}{2}) + \gamma] \frac{\omega}{r_H} + \cdots \approx -e^{-2i[\psi(\frac{\Delta_{\pm}}{2}) + \gamma] \frac{\omega}{r_H}}. \end{aligned} \quad (47)$$

¹⁴If ω is small we are outside the validity of the quasistatic approximation for the collapsing shell case, but here we want to check that all poles converge towards zero. Moreover, the approximation is still valid if we consider the other process which was discussed in the introduction, the "slowed down" collapse at fixed ADM energy.

where the last exponential is introduced for convenience. Then, the two equations (for poles and zeros) can be written in the form

$$\left(\frac{a - ix}{a + ix}\right) e^{ib_{\pm}x} = 1 , \quad (48)$$

or equivalently

$$\frac{x}{a} = \tan\left(\frac{xb_{\pm}}{2}\right) , \quad (49)$$

with

$$x = \omega/r_H , \quad (50)$$

$$b_{\pm} = \ln(u - 1) + 2[\psi(\frac{\Delta_{\pm}}{2}) + \gamma] . \quad (51)$$

As can be easily seen by plotting the functions involved, the equation (49) has an infinite number of real solutions which can be labeled by an integer n . For $1 \ll n \ll \ln((r_s^2 - r_H^2)/r_s^2)$ at leading order the solutions are

$$\frac{\omega}{r_H} \approx -\frac{2\pi n}{\ln[\frac{r_s^2 - r_H^2}{r_H^2}] + 2[\psi(\frac{\Delta_{\pm}}{2}) + \gamma]} , \quad (52)$$

with n an integer, corresponding to values on the real ω axis. This is our result for the poles and zeroes of H in the limit $r_s \rightarrow r_H$. If we choose Δ_+ in (52), we obtain the poles, if Δ_- , we obtain the zeroes. These two do not agree as long as $\Delta_+ \neq \Delta_-$, which is true for $\nu = \sqrt{1 + m^2} > 0$. Note that the solutions are purely real. We commented earlier that as $r_s \rightarrow r_H$, the poles are complex, but flow towards the real axis and the imaginary part quickly becomes many orders of magnitude smaller than the real part. What happened above is that the imaginary part was too small to show up without keeping more subleading terms. In fact keeping the term of order $(\omega/r)^\nu$ in (45) gives rise to a tiny imaginary part, with a sign depending on the boundary conditions used. In the extreme limit, the logarithm in the denominator of (52) begins to dominate more and more over the Δ -dependent term, so the poles and zeroes approach each other, finally cancelling out and converting into a cut on the real axis. In the appendix we give a simple example of how zeroes and poles can form a cut.

4 Discussion

In the previous sections we have shown how, as the shell moves closer to its own horizon, the poles and zeros of the boundary propagator in the complex ω plane accumulate giving rise to a cut. The appearance of the cut is the signal in the boundary theory of the

formation of the black hole horizon in the bulk. It is related to the fact that at the horizon different boundary conditions (ingoing or outgoing waves) are appropriate on different sides of the real ω -axis. In our case these boundary conditions appear automatically when the shell collapses. Once the cut has formed it is meaningful to perform an analytic continuation of the propagator below the real axis and then new poles can appear. In AdS_3 only the thermal poles were found, but if we had performed the calculation in AdS_5 then the poles computed in [19] would have appeared after the collapse of the shell. Let us keep in mind that when we talk about collapse and motion of the shell, it is only within the quasistatic approximation which from the boundary perspective is more akin to a thermodynamic treatment than a true dynamical description.

An open question is that there appears to be two relevant timescales as the shell is approaching the horizon. On one hand, τ , the inverse of the imaginary part of a pole of H , gives a timescale corresponding to the lifetime of the corresponding resonance. On the other hand, the equation of motion for the shell (in this region) was approximately given by the equation (1) with a characteristic timescale

$$\tau_H = 4\pi T_H \sim r_H . \quad (53)$$

It remains to be understood properly which one is the relevant timescale for the thermalization in this case: the lifetime of the resonances, or the time for the collapse, and how the latter could be found in the boundary theory.

Our present understanding is then the following. In the beginning, as the shell is very large, and just begins to collapse, the boundary theory is very far from the thermal equilibrium. The propagator reveals this by having a pole structure which is very different from a thermal propagator. The poles correspond to an infinite tower of resonances in the boundary theory with masses proportional to the shell radius, and lifetimes inversely proportional to it. As the collapse begins to speed up we cannot apply the quasistatic analysis - there will be dynamical processes in the boundary theory which are beyond our control at this stage. However, as a first crude step, we can jump to the very end of the collapse when a far-away observer at a fixed radial distance would see the collapse to slow down and “freeze” as the shell is approaching the horizon radius. At that stage, as a rough approximation, we again apply the quasistatic analysis, in the large frequency domain. Now the boundary theory is approaching thermal equilibrium with deviations encoded in the propagator. The poles and zeroes of the propagator flow towards the real axis of the complex ω -plane, and finally degenerate into a cut with the propagator being the thermal one. The full propagator is then defined either on the upper or lower half plane, corresponding to a choice between a retarded or advanced propagator. A continuation across the cut then reveals the thermal poles on the other half-plane. I.e. $G = -\frac{A_-}{A_+}$ is analytically continued down through the cut into the lower half plane where one finds

the thermal poles. So the propagator has, as promised, become a thermal (retarded or advanced) propagator when the shell is infinitesimally close to the horizon and Hawking radiation begins to leak out and fill the anti-de Sitter space so that a thermal equilibrium is established.

We emphasize that the propagator is just a measure of the properties of the state of the boundary theory. The analysis does not tell us anything about *how* the thermalization happens - there is no dynamical information about the boundary theory. This question is tied up with going beyond the quasistatic approximation, where dynamical issues become relevant. What one would need at that stage, is a kinetic theory for the thermalization of the strongly coupled boundary theory. This seems to be an untractable problem at the moment. One can speculate that the equations governing the thermalization of the boundary theory would be a kinetic theory equivalent of the equations of motion of the collapsing shell in the bulk. That is, if one were to understand the kinetic theory, one should be able to reproduce the equation of the motion of the shell. Further, it has been suggested before [29, 30, 31, 32] that a holographic description of even the simplest dynamical processes in the bulk can be very non-local - even a slightest innocuous looking approximation on the boundary side might completely distort the bulk interpretation. The same could be true about the kinetic theory / shell collapse duality. A small approximation to the kinetic equations might completely mess up the bulk description of the collapse.

Acknowledgments

We thank L. Thorlacius for a useful discussion. The work of U.D. was supported by Swedish Natural Science Research Council (NFR) and that of M.K. by The Swedish Foundation for International Cooperation in Research and Higher Education (STINT).

Appendix

In section 3 we discussed how the series of poles and zeros of the propagator accumulate on the real axis giving rise to a cut. To clarify how this happens we give in this appendix a simpler example in which this occurs. Consider the function

$$G(z) = \frac{\sqrt{\lambda}\Gamma(\lambda z)}{\Gamma(\lambda z + \frac{1}{2})} \quad (54)$$

where λ is a positive real number and $z \in C$. The function $G(z)$ has poles at $z = -n/\lambda$ and zeros at $z = -(n + 1/2)/\lambda$ with n a positive integer. When $\lambda \rightarrow \infty$ the poles and

zeros accumulate on the negative real axis. In that limit and for $-\pi < \arg(z) < \pi$ the Stirling approximation gives

$$\lim_{\lambda \rightarrow \infty} G(z) = \lim_{\lambda \rightarrow \infty} \frac{\sqrt{\lambda} \Gamma(\lambda z)}{\Gamma(\lambda z + \frac{1}{2})} = \lim_{\lambda \rightarrow \infty} \sqrt{\lambda} \frac{(\lambda z)^{\lambda z - 1/2} e^{-\lambda z}}{(\lambda z + 1/2)^{\lambda z} e^{-\lambda z - 1/2}} = \frac{1}{\sqrt{z}} \quad (55)$$

The resulting function, $1/\sqrt{z}$ has a cut which, as follows from the calculation, is placed on the negative real axis. In fact this example arises when taking the large frequency limit of the AdS propagator in global coordinates. In that case one recovers the propagator in Poincaré coordinates which has a cut on the positive real axis.

References

- [1] Juan Maldacena. *The Large N limit of superconformal field theories and supergravity*. *Adv. Theor. Math. Phys.*, 2:231, 1998. [hep-th/9711200](#).
- [2] Ofer Aharony, Steven S. Gubser, Juan Maldacena, Hirosi Ooguri, and Yaron Oz. *Large N field theories, string theory and gravity*. 1999. [hep-th/9905111](#).
- [3] Esko Keski-Vakkuri. *Bulk and boundary dynamics in BTZ black holes*. *Phys. Rev.*, D59:104001, 1999. [hep-th/9808037](#).
- [4] Ulf H. Danielsson, Esko Keski-Vakkuri, and Martin Kruczenski. *Vacua, propagators, and holographic probes in AdS / CFT*. *JHEP*, 01:002, 1999. [hep-th/9812007](#).
- [5] Ulf H. Danielsson, Esko Keski-Vakkuri, and Martin Kruczenski. *Spherically collapsing matter in AdS, holography, and shellons*. 1999. [hep-th/9905227](#).
- [6] Vijay Balasubramanian, Per Kraus, and Albion Lawrence. *Bulk vs. boundary dynamics in anti-de Sitter space-time*. 1998. [hep-th/9805171](#).
- [7] Tom Banks, Michael R. Douglas, Gary T. Horowitz, and Emil Martinec. *AdS dynamics from conformal field theory*. 1998. [hep-th/9808016](#).
- [8] S. W. Hawking. *Breakdown of predictability in gravitational collapse*. *Phys. Rev.*, D14:2460, 1976.
- [9] Yoav Peleg and Alan R. Steif. *Phase transition for gravitationally collapsing dust shells in 2+1 dimensions*. *Phys. Rev.*, D51:3992–3996, 1995. [gr-qc/9412023](#).
- [10] S.F. Ross and R.B Mann. *Gravitationally collapsing dust in 2+1 dimensions*. *Phys. Rev.*, D47:3319, 1993. [hep-th/9208036](#).

- [11] S. W. Hawking and Don N. Page. *Thermodynamics of black holes in anti-de-Sitter space*. *Commun. Math. Phys.*, 87:577, 1983.
- [12] Vijay Balasubramanian, Per Kraus, Albion Lawrence, and Sandip P. Trivedi. *Holographic probes of anti-de Sitter space-times*. 1998. **hep-th/9808017**.
- [13] Gary T. Horowitz and N. Itzhaki. *Black holes, shock waves, and causality in the AdS / CFT correspondence*. *JHEP*, 02:010, 1999. **hep-th/9901012**.
- [14] E. T. Akhmedov, *A Remark on the AdS/CFT Correspondence and the Renormalization Group Flow*. *Phys. Lett.* **B442** (1998) 152. **hep-th/9806217**. E. Alvarez and C. Gomez, *Geometric Holography, the Renormalization Group and the c-theorem*, *Nucl. Phys.* **B541** (1999) 441, **hep-th/9807226**. L. Girardello, M. Petrini, M. Petratti and A. Zaffaroni, *Novel Local CFT and Exact Results on Perturbations of $N=4$ Super Yang-Mills from AdS Dynamics*, **hep-th/9810126**. *The Supergravity Dual of $N=1$ Super Yang-Mills Theory*, **hep-th/9909047**. V. Balasubramanian and P. Kraus, *Space-time and the Holographic Renormalization Group*, *Phys. Rev. Lett.* **83** (1999) 3605, **hep-th/9903190**. M. Petratti and A. Starinets, *RG Fixed Points in Supergravity Duals of 4-d Field Theory and Asymptotically AdS Spaces*, *Phys. Lett.* **B454** (1999) 77, **hep-th/9903241**. D. Z. Freedman, S. S. Gubser, K. Pilch and N. P. Warner, *Renormalization Group Flows from Holography-Supersymmetry and a c-theorem*, **hep-th/9906194**. K. Skenderis and P. K. Townsend, *Gravitational Stability and Renormalization-Group Flow*, **hep-th/9909070**. O. deWolfe, D. Z. Freedman, S.S. Gubser and A. Karch, *Modelling the Fifth Dimension with Scalars and Gravity*, **hep-th/9909134**. **hep-th/9807226**. J. de Boer, E. Verlinde and H. Verlinde, *On the holographic renormalization group*, **hep-th/9912012**.
- [15] L. Susskind and E. Witten. *The Holographic bound in anti-de Sitter space*. 1998. **hep-th/9805114**.
- [16] Amanda W. Peet and Joseph Polchinski. *UV / IR relations in AdS dynamics*. *Phys. Rev.*, D59:065011, 1999. **hep-th/9809022**.
- [17] Vijay Balasubramanian and Simon F. Ross. *Holographic particle detection* 1999. **hep-th/9906226**.
- [18] Steven B. Giddings and Simon F. Ross. *D3-brane shells to black branes on the Coulomb branch* 1999. **hep-th/9907204**.
- [19] Gary T. Horowitz and Veronika E. Hubeny. *Quasinormal modes of AdS black holes and the approach to thermal equilibrium* 1999. **hep-th/9909056**.

- [20] Gary T. Horowitz. *Comments on black holes in string theory* 1999. **hep-th/9910082**.
- [21] S. S. Gubser, I. R. Klebanov, and A. M. Polyakov. *Gauge theory correlators from noncritical string theory*. *Phys. Lett.*, B428:105, 1998. **hep-th/9802109**.
- [22] Edward Witten. *Anti-de Sitter space and holography*. *Adv. Theor. Math. Phys.*, 2:253, 1998. **hep-th/9802150**.
- [23] Daniel Z. Freedman, Samir D. Mathur, Alec Matusis, and Leonardo Rastelli. *Correlation functions in the $CFT(d) / AdS(d+1)$ correspondence*. *Nucl. Phys.*, B546:96, 1999. **hep-th/9804058**.
- [24] S. Kalyana Rama and B. Sathiapalan. *On the role of chaos in the AdS/CFT connection*. 1999. **hep-th/9905219**.
- [25] Hans-Jurgen Matschull. *Black hole creation in (2+1)-dimensions*. *Class. Quant. Grav.*, 16:1069, 1999. **gr-qc/9809087**.
- [26] E. Kiritsis and T.R. Taylor. *Thermodynamics of D-brane probes*. **hep-th/9906048**.
- [27] E. Kiritsis. *Supergravity, D-brane probes and thermal super Yang-Mills: A comparison*. *JHEP* 10:010, 1999. **hep-th/9906206**.
- [28] Ikuo Ichinose and Yuji Satoh. *Entropies of scalar fields on three-dimensional black holes*. *Nucl. Phys.*, B447:340–372, 1995. **hep-th/9412144**.
- [29] Leonard Susskind. *Holography in the flat space limit*. 1998. **hep-th/9901079**.
- [30] Joseph Polchinski, Leonard Susskind and Nicolaos Toumbas. *Negative energy, superluminosity and holography*. *Phys. Rev.*, D60:084006, 1999. **hep-th/9903228**.
- [31] David A. Lowe and Larus Thorlacius. *AdS/CFT and the information paradox*. *Phys. Rev.*, D60:104012, 1999. **hep-th/9903237**.
- [32] Leonard Susskind and Nicolaos Toumbas. *Wilson loops as precursors*. 1999. **hep-th/9909013**.